Self-Organization-Induced Three-Dimensional Honeycomb Pattern in Structure-Controlled Bulky Methacrylate Polymers: Synthesis, Morphology, and Mechanism of Pore Formation

V. D. Deepak and S. K. Asha*

Speciality Polymers, Chemical Sciences & Technology Division, Regional Research Laboratory, Thiruvananthapuram 695019, India

Received: June 5, 2006; In Final Form: July 21, 2006

Here we report, for the first time, a novel molecular design for three-dimensional honeycomb structures through a self-organization of hydrogen-bonded bulky anchoring group in a methacrylic polymer backbone. The polymerizable monomer design includes a methacrylic double bond linked to various hydrophobic anchoring units such as ethane, *n*-decane, tricyclodecane (TCD), and adamantane via a hydrogen-bonded cycloaliphatic urethane linkage. The structures of the polymers were confirmed by nuclear magnetic resonance (NMR) and the molecular weights of the polymer were determined by gel permeation chromatography (GPC). The methacrylate polymers having tricyclodecane and adamantane bulky anchoring groups self-organized to produce three-dimensional honeycomb patterns in tetrahydrofuran−water solvent mixture at ambient conditions, whereas its linear analogues (ethane, *n*-decane) failed to produce any micropattern. The scanning electron microscopy (SEM) analysis of the above-prepared polymer films revealed that the structure of the polymer played a major role in the formation of the honeycomb patterns. The solution Fourier transform infrared (FTIR) measurements confirmed that the bulky tricyclodecane and adamantane polymers have strong hydrogen-bonding interaction compared to that of their linear analogues, which is the driving force for the micropatterns. Transmission electron microscopy (TEM) and atomic force microscopy (AFM) analysis of the bulky polymers revealed that the polymers exist as vesicles or micelles in the solution, which leads to the formation of the honeycomb pattern. The honeycomb pattern formation in the bulky polymer systems suggests that two cooperative factors such as hydrogen-bonding interaction and hydrophobicity of bulky anchoring units are necessary to induce three-dimensional honeycomb structures. To investigate the effect of molecular weights and its distribution on the self-organization process, both benzoyl peroxide (BPO) initiated free radical and atom transfer radical polymerization (ATRP) techniques were employed for the polymerization. Micropores formed irrespective of differences in molecular weight and polydispersity index (PDI); however, the pore size distribution was influenced by both molecular weights and PDI. Low molecular weight samples afforded polydisperse pores with the ATRP samples with more narrow PDI producing pores with large dimensions. The approach has also been investigated for polystyrene-bulky methacrylic copolymer, and the results revealed that uniform honeycomb patterns were produced for copolymers having more than 50 mol % incorporation of bulky units.

Introduction

Self-assembly of polymers leading to microstructures having good morphologies has been an interesting area of research in recent years. Microporous polymers have found interest for their potential applications in diverse areas such as templates for the synthesis of nanoobjects, membranes for selective transport, controlled release of drugs, filters for cell sorting, and also applications in electronic and mechanical devices.[1−5] There are several methods reported for fabricating honeycomb patterned porous polymer films.[6−8] The breath-figure method pioneered recently by Francois and co-workers has received wide acceptance.[9,10] In this method, porous films are prepared by simple casting of polymer solutions of a water-immiscible solvent under high humidity, and upon complete evaporation of the solvent, traces of water droplets remain in the polymer film, which induce honeycomb porous structure. The advantage of this method was that it could be employed to prepare micropatterned surfaces with very large areas.[11−19] Recently, Wang et al. presented a facile method for fabricating polymer thin films with micropatterned surfaces by evaporating polymer solution containing a small amount of water or ethylene glycol in air.[20] Here, the pattern formation was brought about by a combination of phase separation and breath-figure effect. Park and Kim introduced another method for fabricating porous polymer films in a dry environment, and in this method, they used water and a water-miscible solvent like tetrahydrofuran to mimic the humid environment.[21] Most of these above-mentioned routes for pattern formation are based on the processing methodology adopted: film casting under a flow of humid air or phase separation using solvent/nonsolvent combination. It has been found that only specially designed polymers such as rod−coil block copolymers, amphiphilic polymers, comb polymers, and block copolymers give honeycomb structure under humid environment.[22−28] These classes of polymers have a tendency to adopt a spherical shape in solution, which supports

* Author to whom correspondence should be addressed. Fax: 0091-471-2491712; e-mail: asha_syamakumari@yahoo.co.in.

10.1021/jp063469a CCC: $33.50
Published on Web 10/06/2006

the formation of highly ordered structures in films. It is expected that the structure and morphology assumes importance in stabilizing the condensed water/nonsolvent droplet on the volatile polymer solution, which is the key step in the pore formation process. The special molecular architectures such as rod−coil block copolymers, amphiphilic block copolymers, or star polymers that are required for pore formation puts a severe restriction on its utilization because of the synthetic routes used, namely, anionic or controlled radical polymerization. In this context, there are reports where self-assembly involving specific interactions such as hydrogen bonding have been made use of to develop polymeric micelles and hollow spheres on the basis of small molecules and homopolymers.[29−31] The added feature of self-assembly brought about by supramolecular interactions is expected to have dramatic effects on the physical properties of the final polymer. Recently, we reported a series of novel cycloaliphatic acrylic monomers where we found that the self-organization induced by the hydrogen-bonding interaction increased their UV-curing efficiency severalfolds compared to those without hydrogen-bonding units.[32] Deepa and Jayakannan from our laboratory reported another new observation on the formation of porous morphology in the main chain cycloaliphatic polyurethanes; they have found that the increase in the hydrogen-bonding interactions increased the tendency for pore formation.[33]

By combining the structural features of these two different systems, we report here for the first time a unique design for three-dimensional honeycomb pattern in methacrylic polymers bearing hydrogen-bonded urethane and hydrophobic bulky anchoring groups. The backbone of this unique comb polymer carries sidearms that are capable of self-organization by way of hydrogen bond formation. Because of the complexity of the phenomenon, there are still several unanswered questions remaining concerning the role of the polymer structure during the honeycomb pattern formation. The methacrylic polymers were designed in such a way to address many of the fundamental questions on the self-organization polymer chains such as (1) the role of the hydrogen bonding, (2) the hydrophilic−hydrophobic interaction, (3) the effect of molecular weight and its distribution, and (4) the effect of copolymerization. The hydrophobicity of the anchoring unit in the methacrylic polymer was controlled synthetically using terminal units such as ethane, *n*-decane, tricyclodecane (TCD), and adamantane. A cycloaliphatic urethane linkage was chosen because the aliphatic urethane linkages are more thermally stable compared to aromatic counterparts and also it increases the solubility of the resultant polymers for various structural characterizations. Both benzoyl peroxide (BPO) initiated free radical and atom transfer radical polymerization techniques were employed for the synthesis of the novel methacrylate polymers. To study the copolymerization effect, polystyrene-bulky methacrylic random copolymers were synthesized by changing the mole of the monomers from 0 to 100 mol % in the feed in the free-radical polymerization. A control polymer having only bulky unit without hydrogen-bonding urethane linkage was also prepared to investigate the role of hydrogen bonding on the self-organization process. The structures of the polymers were confirmed by NMR spectroscopy, and the hydrogen-bonding interactions were studied by solution FT-IR techniques. The morphology of the polymers was analyzed by scanning electron microscopy (SEM), transmission electron microscopy (TEM), and atomic force microscopy (AFM). Thus, here for the first time, a systematic effort has been taken to understand the structure property relationship of polymers in the formation of highly ordered honeycomb films.

Experimental Section

Materials. Isophorone diisocyanate (IPDI), 2-hydroxyethyl methacrylate (HEMA), dibutyltin dilaurate (DBTDL), adamantanemethanol, ethyl-2-bromo propionate, and 2,2′-bipyridine (bpy) were purchased from Sigma Aldrich and were used without further purification. CuBr (98%, Aldrich) was stirred in glacial acetic acid overnight, was filtered, and then was washed with ethanol and was dried under vacuum at 60 °C overnight. 8-Hydroxymethyltricyclo[5.2.1.$0^{2,6}$]decane (tricyclodecane methanol) was obtained from Celanese Chemicals and was used as such. Decanol was purchased from Merck, Germany and was used as such. Benzoyl peroxide (BPO), tetrahydrofuran (THF), *N*,*N*-dimethyl formamide (DMF), and ethanol were purchased locally and were purified using standard procedures.

Instrumentation. NMR spectra of the compounds were recorded using 300-MHz Brucker NMR spectrophotometer in $CDCl_3$ containing a small amount of tetramethylsilane (TMS) as internal standard. Infrared spectra of the polymers were recorded using an IRPrestige-21 FT-IR Shimadzu spectrophotometer in the range of 4000−400 cm^{-1}. The purity of the compounds was determined by JEOL JSM600 fast atom bombardment (FAB) high-resolution mass spectrometry. The molecular weights of the polymers were determined by GPC in THF using polystyrene standards for the calibration. Waters 510 pump connected through three series of Styragel HR columns (HT-3, HT-4, and HT-5) and Waters 410 differential refractometer was used for analyzing the samples. The flow rate of the THF was maintained as 1 mL throughout the experiments, and 1 wt % of (10 mg in 1 mL) the polymer was filtered and injected for recording the GPC chromatograms at 30 °C. The thermal stability of the polymers was determined using DTG-60 Shimadzu thermogravimetric analyzer at a heating rate of 10 °C/min in nitrogen. For SEM measurements, polymer samples were provided with a thin gold coating using JEOL JFC-1200 fine coater. The probing side was inserted into JEOL JSM-5600 LV scanning electron microscope for taking photographs. The sample preparation method adopted was as follows. A solvent/nonsolvent mixture of THF/water was first mixed in a 9:1 ratio, and then 10 mg of polymer was dissolved in 1 mL of this mixture resulting in a stable and clear polymer solution. A drop of this solution was placed on a clean glass slide and was allowed to evaporate slowly in air. All films were prepared at atmospheric pressure without air flow. Atomic force microscopy images were recorded under ambient conditions using a Digital Instrument Multimode Nanoscope IV operating in the tapping mode regime. Microfabricated silicon cantilever tips (MPP-11100-10) with a resonance frequency of 299 kHz and a spring constant of 20−80 N m^{-1} were used. The scan rate varied from 0.5 to 1.5 Hz. AFM section analysis was done offline. Samples were prepared by depositing one drop of the filtered polymer solution (10^{-6} M solution of sample in THF/water = 9:1 mixture) onto a freshly cleaved mica sheet. Transmission electron microscope (TEM) images were recorded using a Hitachi H-600 instrument at 75 KV. For TEM measurements, a drop of the polymer solution (10 mg in 1 mL of THF/water = 9:1 mixture) was deposited directly on Formvar coated copper grid.

Synthesis of 2-Methyl-acrylic Acid 2-[1,3,3-Trimethyl-5-(tricyclo[5.2.1.$0^{2,6}$] decylmethoxycarbonylamino)-cyclohexylmethylcarbamoyloxy]-ethyl Ester (TCDM-Monomer). Isophorone diisocyanate (IPDI) (6 g, 0.027 mol) in 20 mL of dry DMF was taken in a 100-mL two-necked round-bottom flask, and the contents were cooled with ice. Hydroxyethyl methacrylate (HEMA) (3.51 g, 0.027 mol) was added dropwise with

constant stirring under nitrogen. The reaction was allowed to proceed under ice cold conditions for half an hour followed by room-temperature stirring for 2 h. Six drops of dibutyltin dilaurate (DBTDL) was added as catalyst followed by dropwise addition of tricyclodecane monomethanol (4.48 g, 0.027 mol) under ice cold condition. It was left stirring in ice for a further half an hour and then was heated to 60 °C for 6 h. The contents were poured into 300 mL of water and were extracted with dichloromethane. The extract was washed with water, dried over anhydrous sodium sulfate, concentrated, and dried in a vacuum oven at 60 °C for 12 h. Yield: 11.8 g (92%). ^{1}H NMR (300 MHz, $CDCl_3$) δ ppm: 6.04, 5.49 (2s, 2H, C**H**$_2$═C), 5.25−4.79 (m, N**H**), 4.25 (s, 4H, O−C**H**$_2$−C**H**$_2$−O of HEMA), 4.01 (m, 2H, −OC**H**$_2$ next to tricyclodecane ring), 3.21 (b, 1H, C**H**−NH−COO of IPDI), 2.86 (b, 2H, −C**H**$_2$−NH−COO of IPDI), 2.32 (b, 2H, tricyclodecane ring), 1.95 (s, 3H, C**H**$_3$− of HEMA), 2.04−0.87 (aliphatic protons of IPDI and tricyclodecane ring). ^{13}C NMR (75 MHz, $CDCl_3$) δ ppm: 166.83, 156.36, 155.13, 135.61, 125.75, 68.16, 67.88, 62.65, 62.21, 61.96, 54.55, 45.14, 44.81, 43.04, 40.87, 39.71, 35.93, 34.74, 33.79, 31.47, 28.63, 27.35, 26.35, 25.95, 22.92, 18.38. FT-IR (cm^{-1}): 3345, 2952, 1715, 1635, 1538, 1456, 1407, 1385, 1365, 1305, 1243, 1170, 1033, 945, 891, 815, 773, 737, 703, 651. (MW: 518) FAB−HRMS m + 1: 519.44.

2-Methyl-acrylic Acid 2-(5-Ethoxycarbonylamino-1,3,3-trimethylcyclohexylmethylcarbamoyloxy)-ethyl Ester (Et-Monomer). Isophorone diisocyanate (IPDI) (6 g, 0.027 mol), hydroxyethyl methacrylate (HEMA) (3.51 g, 0.027 mol), and ethanol (1.2 g, 0.027 mol) were used, and the rest of the procedures are the same as described for TCDM-monomer. Yield: 9.8 g (91%). ^{1}H NMR (300 MHz, $CDCl_3$) δ ppm: 6.04, 5.49 (2s, 2H, C**H**$_2$═C), 5.22−4.73 (m, N**H**), 4.23 (s, 4H, O−C**H**$_2$−C**H**$_2$−O of HEMA), 4.01 (m, 2H, −OC**H**$_2$−CH_3 of ethanol), 3.69 (b, 1H, C**H**−NH−COO of IPDI), 2.82 (b, 2H, −C**H**$_2$−NH−COO of IPDI), 1.85 (s, 3H, C**H**$_3$− of HEMA), 1.64−0.79 (aliphatic protons of IPDI). ^{13}C NMR (75 MHz, $CDCl_3$) δ ppm: 166.98, 156.98, 155.82, 135.76, 125.79, 62.74, 60.54, 60.31, 54.63, 46.84, 46.13, 44.29, 41.66, 36.19, 34.85, 31.61, 27.41, 23.01, 18.05, 14.43. FT-IR (cm^{-1}): 3331, 2954, 1717, 1634, 1534, 1462, 1382, 1303, 1243, 1171, 1044, 949, 902, 814, 776, 650. (MW: 398) FAB−HRMS m + 1: 399.32

2-Methyl-acrylic Acid 2-(5-Decyloxy carbonylamino-1,3,3-trimethylcyclohexylmethylcarbamoyloxy)-ethyl Ester (Dec-Monomer). Isophorone diisocyanate (IPDI) (6 g, 0.027 mol), hydroxyethyl methacrylate (HEMA) (3.51 g, 0.027 mol), and *n*-decanol (4.27 g, 0.027 mol) were used, and the rest of the procedures are the same as described for TCDM-monomer. Yield: 12.5 g (91%).^{1}H NMR (300 MHz, $CDCl_3$) δ ppm: 5.99, 5.44 (2s, 2H, C**H**$_2$═C), 5.41−4.62 (m, N**H**), 4.17 (s, 4H, O−C**H**$_2$−C**H**$_2$−O of HEMA), 3.88 (m, 2H, −OC**H**$_2$ of decanol), 3.63 (b 1H, C**H**−NH−COO of IPDI), 2.78 (b, 2H, −C**H**$_2$−NH−COO of IPDI), 1.79 (s, 3H, C**H**$_3$− of HEMA), 1.55−0.72 (aliphatic protons of IPDI and decanol). ^{13}C NMR (75 MHz, $CDCl_3$) δ ppm: 166.61, 157.99, 155.75, 135.54, 125.49, 64.48, 64.27, 62.57, 61.79, 54.49, 46.91, 45.86, 44.27, 41.31, 36.01, 34.65, 31.33, 29.09, 28.85, 27.18, 25.02, 22.81, 21.95, 17.78, 13.64. FT-IR (cm^{-1}): 3335, 2922, 1715, 1635, 1538, 1458, 1305, 1242, 1171, 1045, 942, 891, 814, 774, 737, 655. (MW: 510) FAB−HRMS m + 1: 511.44.

2-Methyl-acrylic Acid 2-[5-(Adamantan-1-ylmethoxycarbonylamino)-1,3,3-trimethyl-cyclohexylmethylcarbamoyloxy]-ethyl Ester (AdM-Monomer). Isophorone diisocyanate (IPDI) (6 g, 0.027 mol), hydroxyethyl methacrylate (HEMA) (3.51 g, 0.027 mol), and adamantanemethanol (4.48 g, 0.027 mol) were used, and the rest of the procedures are the same as described for TCDM-monomer. Yield: 11.9 g (93%). ^{1}H NMR (300 MHz, $CDCl_3$) δ ppm: 6.04, 5.50 (2s, 2H, C**H**$_2$═C), 5.22−4.73 (m, N**H**), 4.21 (s, 4H, O−C**H**$_2$−C**H**$_2$−O of HEMA), 3.66−3.55 (b, 3H, −OC**H**$_2$ next of AdM ring and −C**H**−NH−COO of IPDI), 3.09−2.82 (b, 2H, −C**H**$_2$−NH−COO of IPDI), 1.86−0.83 (aliphatic protons of IPDI and adamantane ring). ^{13}C NMR (75 MHz, $CDCl_3$) δ ppm: 167.03, 156.47, 155.31, 135.75, 125.90, 74.36, 73.48, 62.77, 62.45, 62.18, 54.69, 53.92, 46.80, 45.77, 44.53, 41.71, 39.08, 38.94, 37.01, 36.82, 36.22, 34.94, 33.17, 31.64, 28.21, 28.01, 27.50, 23.15, 18.05. FT-IR (cm^{-1}): 3366, 2903, 1715, 1635, 1538, 1452, 1300, 1242, 1167, 1038, 938, 812, 772, 652. (MW: 518) FAB−HRMS m + 1: 519.55.

Synthesis of Control Monomer (Tricyclo[5.2.1.0^{2,6}]-decylmethyl Methacrylate).[34] Tricyclo[5.2.1.0^{2,6}]decane methanol (10.0 g, 0.06 mol) in 25 mL toluene was taken in a 100-mL two-necked round-bottom flask. Then, *p*-toluene sulfonic acid (0.3 g, 0.0015 mol), methacrylic acid (6 mL, 0.068 mol), and a pinch of hydroquinone were added. The flask was then connected to the Dean Stark apparatus and to a water condenser and was heated to a temperature of 125 °C with stirring for 19 h. The contents were poured into 150 mL of water and then were extracted with 20 mL toluene, were washed with sodium bicarbonate solution, and then were washed with brine. Finally, it was filtered and dried in a vacuum oven for 12 h. Yield: 9.2 g (65%). ^{1}H NMR (300 MHz, $CDCl_3$) δ ppm: 6.09 (s, 2H, C**H**$_2$═C), 5.54 (s, 2H, C**H**$_2$═C), 3.86 (d, 2H, −OC**H**$_2$), 2.42 (m, 2H), 2.13 (m, 3H), 1.94 (s, 3H, −C**H**$_3$), 1.67−1.41 (m, 9 H), 0.96 (m, cycloaliphatic protons). ^{13}C NMR (75 MHz, $CDCl_3$) δ ppm: 167.51, 136.57, 124.98, 68.18, 45.55, 45.14, 43.72, 41.25, 40.02, 33.85, 28.92, 27.69, 26.89, 26.41, 18.24. FT-IR (cm^{-1}): 3420, 2950, 1720, 1638, 1470, 1453, 1403, 1376, 1354, 1317; 1295, 1167, 1083, 1013, 978, 937, 893, 858, 815, 730, 695, 654, 601, 527, 481. (MW: 234) FAB−HRMS m + 1: 235.34.

Atom Transfer Radical Polymerization (ATRP) of Methacrylic Monomers. Ethyl-2-bromopropionate (0.014 g, 7.72×10^{-5} mol) was added to a round-bottom flask containing Cu(I)Br (0.011 g, 7.72×10^{-5} mol), bipyridyl (0.024 g, 1.54×10^{-4} mol), and TCDM-monomer (1 g, 1.9×10^{-3} mol) in 5 mL THF. The flask was sealed with rubber septum and was purged with nitrogen for 20 min before adding the initiator. The septum was replaced with a water condenser, and then it was heated in an oil bath at 65 °C for 6 h under nitrogen atmosphere. The viscous liquid was dissolved in THF and was passed through a silica column to remove the copper catalyst and then was concentrated and precipitated in methanol. Yield: 0.72 g (72%). ^{1}H NMR (300 MHz, $CDCl_3$) δ ppm: 5.69−5.13 (b, N**H**), 4.21 (b, 4H, O−C**H**$_2$−C**H**$_2$−O of HEMA), 3.72 (b, 2H, −OC**H**$_2$ next to tricyclodecane ring), 3.41−2.85 (b, 3H, C**H**$_2$−NH−COO, and C**H**−NH−COO of IPDI), 2.31 (b, 2H of tricyclodecane ring), 2.03−0.86 (m, 33 H, others). ^{13}C NMR (75 MHz, $CDCl_3$) δ ppm: 177.74, 157.57, 155.63, 68.68, 63.62, 61.71, 54.95, 45.65, 45.32, 43.74, 41.35, 40.22, 36.54, 35.32, 34.29, 31.97, 29.13, 27.86, 27.10, 26.63, 23.33. FT-IR (KBr, cm^{-1}): 3386, 2952, 1720, 1529, 1462, 140, 1387, 1350, 1307, 1240, 1154, 1055, 965, 864, 773.

The other polymers were synthesized using the same procedure using 1.0 g of respective monomers instead of TCDM-monomer.

PolyEt. Yield: 0.86 g (86%).^{1}H NMR (300 MHz, $CDCl_3$) δ ppm: 4.74−4.6 (b, N**H**), 4.10 (b, 4H, O−C**H**$_2$−C**H**$_2$−O of HEMA), 3.73 (b, 2H, −OC**H**$_2$−CH_3 of ethanol), 3.31−2.91 (b,

SCHEME 1: Synthesis of Monomers

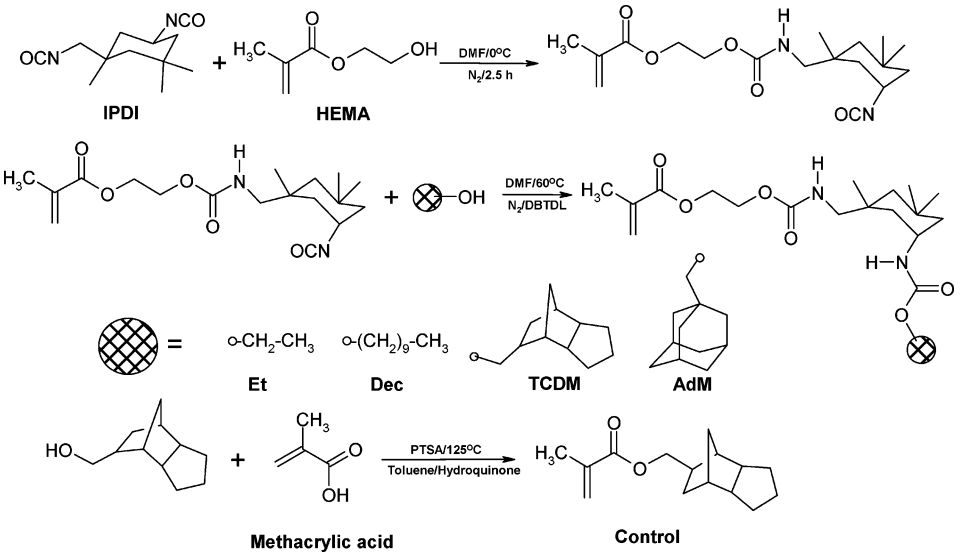

3H, C**H**$_2$−NH−COO, and C**H**−NH−COO of IPDI), 2.34−0.926 (m, 23H, others). ^{13}C NMR (75 MHz, $CDCl_3$) δ ppm: 177.38, 156.99, 155.84, 60.68, 54.72, 46.96, 46.28, 44.42, 41.81, 36.26, 34.94, 31.73, 29.48, 29.36, 27.52, 23.09, 14.53. FT-IR (KBr, cm^{-1}): 3380, 2956, 1719, 1537, 1462, 1387, 1308, 1243, 1154, 1048, 963, 866, 776.

PolyDec. Yield: 0.85 g (85%). ^{1}H NMR (300 MHz, $CDCl_3$) δ ppm: 4.37−4.16 (b, N**H**), 3.95 (b, 4H, O−C**H**$_2$−C**H**$_2$−O of HEMA), 3.72 (b, 2H, −OC**H**$_2$ of decanol), 2.92−2.83 (b, 3H, C**H**$_2$−NH−COO, and C**H**−NH−COO of IPDI), 2.26−0.79 (m, 39H, others). ^{13}C NMR (75 MHz, $CDCl_3$) δ ppm: 178.01, 157.38, 156.34, 65.24, 65.01, 54.95, 47.20, 46.52, 44.65, 42.02, 36.49, 35.17, 32.00, 29.66, 29.42, 29.17, 27.74, 26.01, 23.32, 22.79, 14.24. FT-IR (KBr, cm^{-1}): 3369, 2925, 1718, 1534, 1461, 1382, 1305, 1242, 1144, 1054, 963, 864, 774.

PolyAdM. Yield: 0.73 g (73%). ^{1}H NMR (300 MHz, $CDCl_3$) δ ppm: 5.22−4.81 (b, N**H**), 4.23 (b, 4H, O−C**H**$_2$−C**H**$_2$−O of HEMA), 3.66 (b, 2H, −OC**H**$_2$ next to AdM ring), 3.46−2.87 (b, 3H, C**H**$_2$−NH−COO, and C**H**−NH−COO of IPDI), 1.96−0.93. (m, 35H, others) Solubility was not enough for recording ^{13}C spectra in $CDCl_3$ alone. ^{13}C NMR (75 MHz, trifluoroacetic acid/$CDCl_3$) δ ppm: 160.94, 159.81, 68.36, 45.38, 39.30, 37.03, 34.71, 31.85, 28.13, 25.57. FT-IR (KBr, cm^{-1}): 3389, 2953, 1723, 1542, 1463, 1386, 1308, 1243, 1155, 1056, 965, 866, 773.

Free-Radical Polymerization of Methacrylic Monomers. TCDM-monomer (1.0 g, 2.9×10^{-3} mol) and benzoylperoxide (0.014 g, 5.7×10^{-5} mol) were taken in THF (5 mL) in a 10-mL round-bottomed flask provided with a water condenser. The reaction mixture was purged with nitrogen for 10 min. The polymerization was carried out by stirring the contents at 65 °C for 8 h. The viscous liquid was cooled and precipitated into methanol. Yield: 0.72 g (72%). The NMR and FT-IR data for all the polymers were identical to that of reported for ATRP route.

Control Polymer. Tricyclo[5.2.1.0^{2,6}]decylmethyl methacrylate (1.0 g, 4.2×10^{-3} mol) was polymerized as described above to obtain the control polymer. Yield: 0.79 g (79%). ^{1}H NMR (300 MHz, $CDCl_3$) δ ppm: 3.71 (s, b, 2H, −OC**H**$_2$), 2.41 (s, b, 2H), 2.13−1.49 (m, 14H), 1.25−0.89 (m, 4H). ^{13}C NMR (75 MHz, $CDCl_3$) δ ppm: 177.62, 68.73, 45.63, 45.20, 44.75, 43.85, 41.29, 40.14, 33.39, 29.09, 28.02, 26.95, 26.48, 18.17, 16.59. FT-IR (KBr, cm^{-1}): 2949, 1718, 1451, 1377, 1314, 1295, 1166, 1059, 1012, 973, 938, 757, 707.

Copolymer Synthesis. A 1:1 copolymer of TCDM-monomer with styrene was synthesized using BPO as the initiator in THF as solvent by taking 50:50 feed ratios of TCDM-monomer (2.07 g, 4×10^{-3} mol) and styrene (0.42 g, 4×10^{-3} mol) under similar conditions as that used for the homopolymer synthesis. Yield: 0.71 g (28%) ^{1}H NMR (300 MHz, $CDCl_3$) δ ppm: 7.11−6.5 (b, 5H, **Ar**−**H**), 4.31 (b, N**H**), 3.88 (b, 4H, O−C**H**$_2$−OC**H**$_2$−O of HEMA), 3.72 (b, 2H, −OC**H**$_2$ next to tricyclodecane ring), 3.41−2.83 (b, 3H, C**H**$_2$−NH−COO, and C**H**−NH−COO of IPDI), 2.41 (b, 2H of tricyclodecane ring), 2.16−0.19 (m, 36 H, others). FT-IR (KBr, cm^{-1}): 3384, 2951, 1726, 1599, 1526, 1453, 1385, 1303, 1236, 1198, 1116, 1056, 902, 864, 761.

Results and Discussion

The monomers were prepared in one pot by selective end capping of isophorone diisocyanate (IPDI) on one side by reacting it with one equivalent of hydroxyethyl methacrylate (HEMA), which was followed by means of FT-IR. This was followed by coupling with one equivalent of various alcohols such as ethanol (Et), *n*-decanol (Dec), tricyclodecanemethanol (TCDM), or adamantanemethanol (AdM) (see Scheme 1). A control monomer was also synthesized by esterification route.[34] The monomers were structurally characterized by means of ^{1}H, ^{13}C NMR, and FTIR spectroscopy. Figure 1a shows the proton

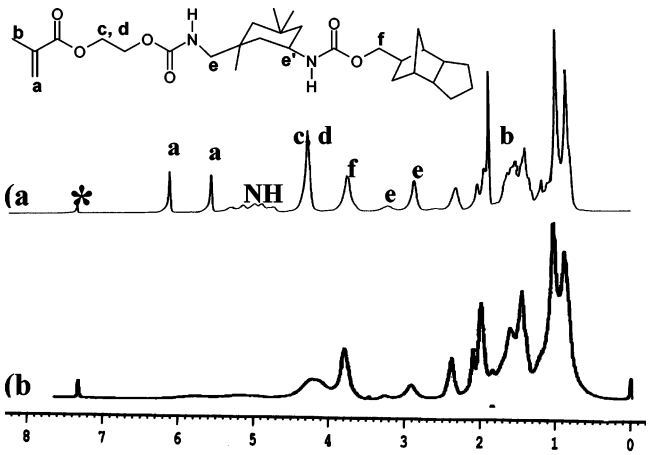

Figure 1. ^{1}H NMR spectra of TCDM-monomer (a) and its polymer (b).

SCHEME 2: Structure of Polymers

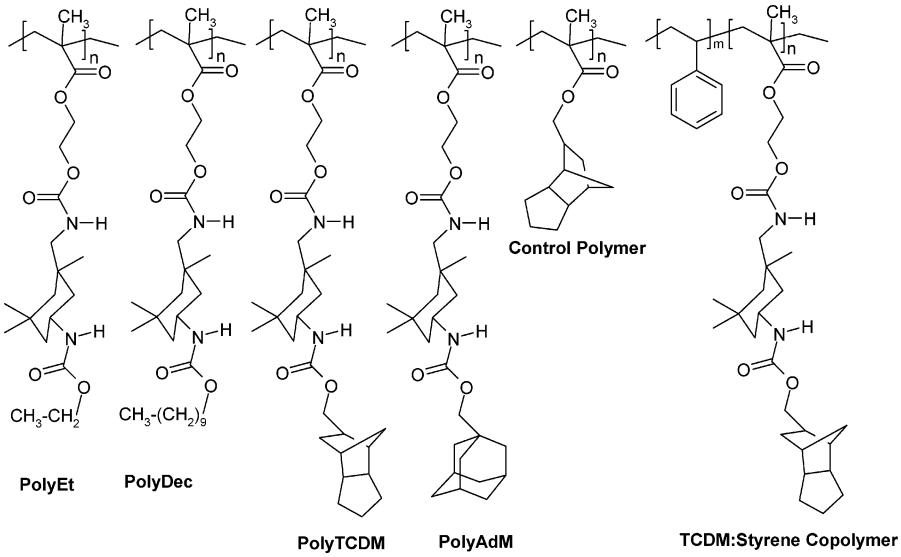

NMR spectra of the TCDM-monomer recorded in $CDCl_3$ with the peaks labeled. The sharp, well-separated peaks at 6.04 and 5.49 ppm, labeled "a", corresponds to the methacrylic double bond protons. The NH proton peaks ~5 ppm appears complicated, because IPDI is a mixture of cis and trans isomers. The $-OC\mathbf{H}_2$ peaks labeled "f" corresponding to the $-OC\mathbf{H}_2$ next to the tricyclodecane unit appears at 4.01 ppm which matches perfectly in intensity with the double bond methacrylic peaks signifying that the different halves of the molecule have coupled stoichiometrically as expected. The normal free-radical polymerization of the monomers was carried out by using 3 mol % benzoyl peroxide (BPO) as initiator in tetrahydrofuran (THF) as solvent. The viscous liquid was cooled and precipitated into methanol in the case of polyTCDM, polyAdM, and control-polymer and water in the case of polyEt and polyDec. Similarly, all the monomers were subjected to controlled radical polymerization via the atom transfer radical polymerization (ATRP) route also using ethyl-2-bromopropionate/CuBr/bipyridyl/monomer in a 1:1:2:25 ratio according to literature procedure.[35,36] Scheme 2 shows the structure of all the polymers. Figure 1 also compares the proton NMR spectra of TCDM-monomer (a) with its polymer (b) indicating the disappearance of the methacrylic double bonds. Additionally, a copolymer of TCDM monomer with styrene was prepared using 3 mol % BPO under identical conditions as that for the homopolymer of TCDM and is given in Scheme 2. From the proton NMR spectra of the copolymer (given in Supporting Information), the extent of incorporation of TCDM was determined on the basis of the integration of peaks at 7.1 and 6.5 ppm which corresponded to the five aromatic protons of styrene as well as the peak at 2.41 ppm which corresponded to two protons of the tricyclodecane ring. The incorporation was found to be more or less similar to the feed ratio with the ratios for TCDM:styrene being 54:46 in the copolymer. The molecular weight details of all the polymers synthesized by both routes, ATRP conditions as well as normal free-radical polymerization using BPO, are given in Tables 1 and 2, respectively. The tables also indicate the number (n) of monomer units incorporated for each polymer, calculated from the molecular weight. In the case of ATRP samples, it can be seen that only for the polyEt and polyDec, the theoretical and obtained molecular weights are similar. In the case of the ATRP samples of the bulky polyTCDM and polyAdM as well as the control-polymer, the number of monomer units incorporated is very much higher than what is theoretically expected.[37] In all cases, the incorporation is very high for the BPO initiated polymerization compared to that of ATRP. Figure 2 shows the GPC chromatograms of polymers prepared by ATRP.

TABLE 1: Yield and Molecular Weight Data of Polymers Prepared via ATRP[a]

polymer	yield[b] (%)	$M_{n,theo}$	n^c theo	M_n (GPC)	PDI	n^c	10 wt % loss temperature (°C)[d]	size of pores (μm)[e]
polyEt	86	8500	20	7200	1.20	18	218	
polyDec	85	10 800	20	9700	1.32	19	270	
polyTCDM	72	9300	18	20 500	1.37	40	284	5−12
polyAdM	73	9400	18	15 500	1.34	30	267	2.5−5
control	79	4600	20	7900	1.33	34		

[a] ATRP conditions: ethyl-2-bromo propionate/CuBr/bipyridyl/monomer = 1:1:2:25. [b] Calculated for isolated products. [c] Number of monomer units incorporated calculated from the respective molecular weights. [d] Determined by thermogravimetric analysis. [e] Calculated from SEM images.

TABLE 2: Yield and Molecular Weight Data of Normal Free Radically Polymerized Samples[a]

polymer	yield[b] (%)	M_n	PDI	n^c	size of pores SEM (TEM) (μm)[d]
polyEt	84	29 600	2.97	70	
polyDec	81	21 700	2.61	40	
polyTCDM	72	16 000	1.57	30	0.7−1.5 (0.6−2.5)
polyAdM	70	28 700	1.69	55	1.5−5 (0.2−0.8)
control	77	26 900	3.33	115	
copoly(TCDM:styrene)	28	40 000	2.73		1−3

[a] Free-radical polymerization conditions: 3 mol % benzoyl peroxide. [b] Calculated for isolated products. [c] Number of monomer units incorporated calculated from the respective molecular weights. [d] Calculated from SEM and TEM images.

The polymer films for SEM micrograph analysis were prepared by dissolving 10 mg of each polymer (free radically polymerized as well as by ATRP route) in 1 mL of THF:water (9:1 v/v) solvent combination and by drop-casting on glass substrates and allowing to evaporate under atmospheric conditions. Spontaneous pore formation was observed for the polyTCDM and polyAdM polymerized using 3 mol % BPO as well as under ATRP route and also for the copolymer of TCDM with styrene, copoly(TCDM:styrene) = 50:50 polymerized using 3 mol % BPO. These observations were perfectly reproducible, and films of each of the samples prepared on different occasions under identical conditions gave similar pore dimensions in their

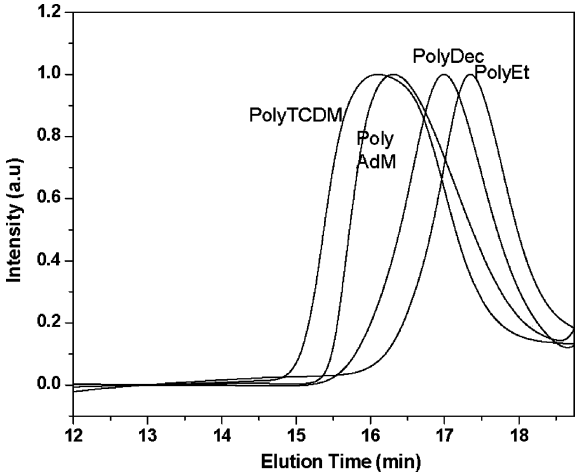

Figure 2. GPC chromatograms of polyTCDM, polyAdM, polyDec, and polyEt prepared via ATRP.

SEM micrographs. Observation under the optical microscope (data not shown) also revealed the honeycomb patterns produced by these polymers. No pattern was observed under the optical microscope for polyTCDM, polyAdM, and the copolymer when their films were cast from THF or chloroform alone. A very poor pore distribution was observed in films cast from THF: water mixture with more water content like THF:water = 8:2 mixture. No special morphology was observed for the films of polyEt, polyDec, and the control-polymer prepared under any of the above-mentioned conditions. They gave thin transparent glassy films whereas polyTCDM, polyAdM, and the copoly-(TCDM:styrene) gave peelable, opaque, brittle films in the THF: water 9:1 mixture. Reports are available in the literature for the influence of the extent of nonsolvent (water) used on pore formation. Wang et al. have shown that larger amounts of water in the THF:water combination leads to larger pore dimensions.[20] In presence of larger water content, water droplets begin to form earlier and they have more time to grow. In the case of bulky methacrylates discussed here, at larger water contents, very poor pore distribution was found, probably because of coalescence and merging of larger pores. Thus, a THF:water combination of 9:1 was found to be optimum for pore formation. A typical SEM micrograph of polyTCDM prepared by polymerization in the presence of 3 mol % BPO (Figure 3a) and prepared under controlled polymerization conditions of ATRP (Figure 3b) is given in Figure 3. Densely packed circular and elongated pores with diameters in the range of 0.7−1.5 μm are visible for the free-radical sample, whereas the ATRP sample had much larger pore diameters in the range of 5−12 μm with the wall thickness ~1.5−2.0 μm. The top view of the polyTCDM films clearly displays the presence of mutually connected spherical cavities throughout the entire bulk. The morphology of the polyAdM films prepared using BPO and using ATRP route are given in Figure 3c and 3d, respectively. The free radically polymerized sample (Figure 3c) had pores with diameter ranging from 1.5 to 5.0 μm, and the ATRP sample (Figure 3d) had pore size in the range of 2.5−5 μm with a wall thickness of ~0.9−1.1 μm. Figure 4 shows the SEM micrographs for the drop-cast film of 50:50 copolymer of TCDM with styrene prepared under identical conditions. Compared with the homopolymer of TCDM, the 50:50 copolymer with styrene gave more uniform and circular densely packed pores having a diameter of 1−3 μm. Generally, controlled polymerization techniques such as the ATRP which give polymers with narrow molecular weight distribution are used to generate porous materials. Here, we have shown that simple free-radical polymerization using thermal initiators such as BPO can also be used to generate porous materials. Molecular weight has been shown to exert a decisive influence on porous pattern makeup in the case of polystyrene with molecular weight ranging from $4800 < M_w < 2\,800\,000$.[38] In that example, bimodal pore size distribution was seen for low molecular mass polystyrene, where large molecular mass polymer gave more homogeneous pore size distribution and the

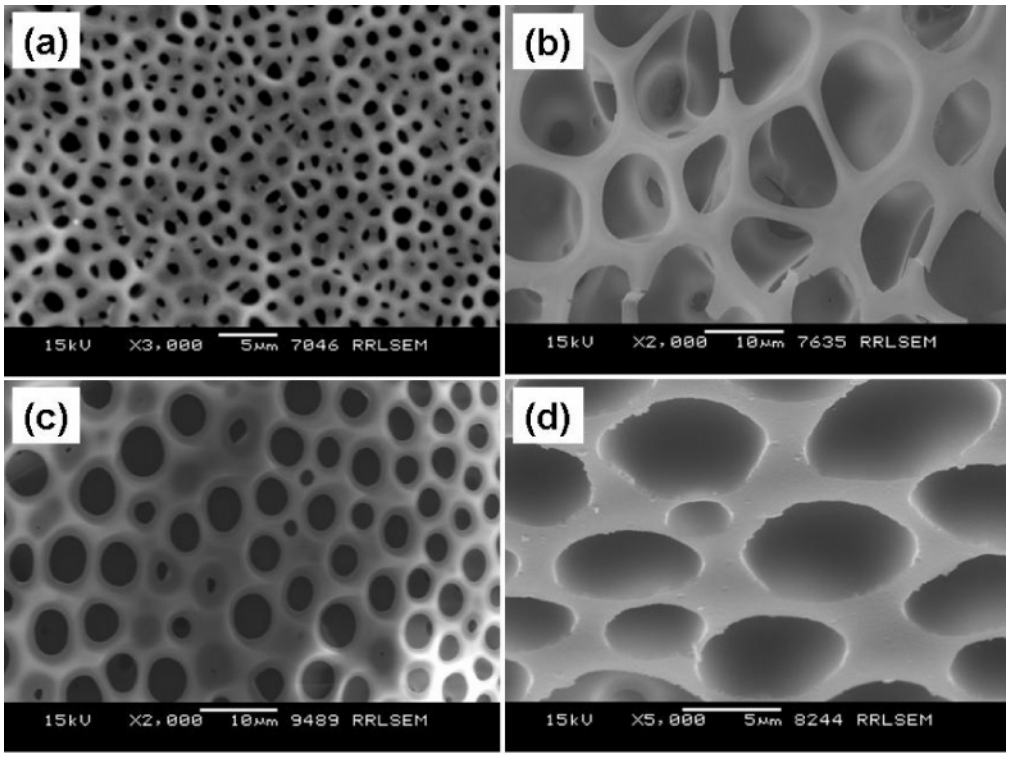

Figure 3. SEM images of polyTCDM [prepared via free radically (a) and ATRP (b)], and polyAdM [prepared via free radically (c) and ATRP (d)]. The films were prepared by drop-casting polymer solution (10 mg/mL) of THF:water (9:1 v/v).

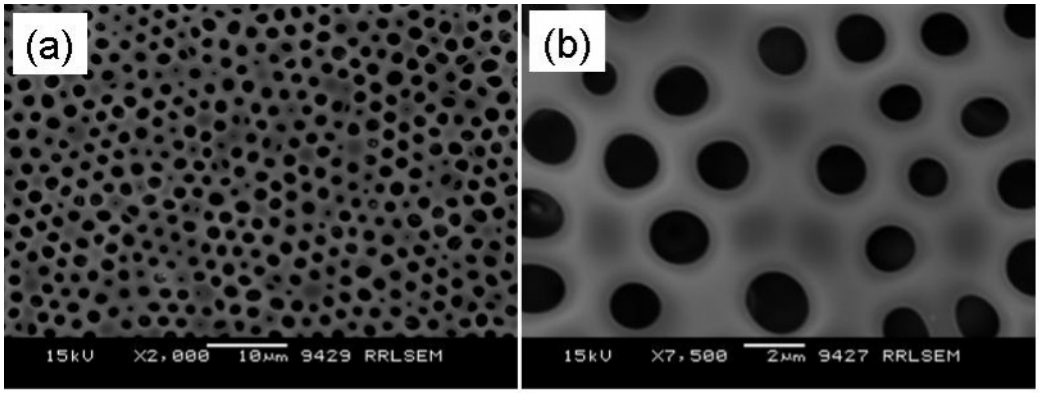

Figure 4. SEM images of copolymer of TCDM:styrene (50:50) in low (a) and high (b) magnification. The films were prepared by drop-casting polymer solution (10 mg/mL) of THF:water (9:1 v/v).

pore size increased with increase in polymer molecular weight. In the present case, the molecular weight, especially that of the homopolymers, lies in the low molecular mass range of 20 700 $< M_w <$ 48 500. Only the copolymer of TCDM:styrene had relatively large M_w of 109 000, and it had a more uniform pore size distribution with local hexagonal ordering. In the case of the homopolymers, mostly polydisperse pores were produced, with narrow PDI samples (via ATRP) producing pores of slightly large dimensions. However, since the molecular weight lies in a quite narrow range, it is difficult to observe any regular trend in the pore pattern. For a thorough understanding of the effect of molecular weight and PDI on pore size distribution and pore pattern, a wider range of molecular weight for the polymer samples would be desirable. The control-polymer as well as polyEt and polyDec prepared under identical conditions did not show any significant features in their SEM images. The examples shown here provide an insight into the important role of the polymer structure on the micropore formation ability of the system. The replacement of the terminal bulky units by alkyl chains, either short (polyEt) or long (polyDec), completely removed the micropore formation ability of the system. The control-polymer, on the other hand, possessed the bulky terminal unit but lacked the other structural features such as the urethane linkage capable of self-organization via hydrogen bonding or ethyleneoxy unit capable of introducing a hydrophilic interaction. The nature of the pores formed, in terms of polydispersity and circular or elongated nature, also is influenced by the polymer structure. Comparing the pattern formed by the homopolymer polyTCDM with that formed by its 50:50 copolymer with styrene, the additional rigidity as well as the hydrophilic/hydrophobic balance afforded by the styrene results in a better balance between the rigid and flexible units in the copolymer leading to a much better control of pore size in the latter case. There are reports in the literature showing that the conditions of film preparation like the sample concentration, humidity, temperature, mode of film preparation, and molecular weight of polymer tremendously influence the nature and type of micropore formation.[38−40] However, in our experiments, except for molecular weight of polymer, the other factors have been maintained constant and have followed the same conditions of film preparation to study the effect of polymer structure on the morphology of films formed.

To further elucidate the morphology of the pores formed, transmission electron microscopic (TEM) characterization was carried out since it is a powerful and efficient technique for revealing the internal microstructure of microparticles. Figure 5 shows the TEM micrographs of BPO polymerized samples of polyAdM (a and b) and polyTCDM (c and d) prepared by drop-casting (10 mg/mL) solution from THF:H_2O = 9:1 v/v onto Formvar coated copper grid without any special staining applied. Therefore, the contrast observed is due to diffraction and phase contrast of the samples themselves. A close examination of polyAdM (Figure 5a and b) shows that it forms spherical polydisperse micellar particles with sizes ranging from 200 nm to 0.8 μm. In Figure 5a and b, the small spheres are seen surrounded by a halo with core of diameter 160−240 nm and shell thickness 40 nm. On the basis of similar observation of TEM images in the literature, the dark images in the middle can be ascribed to the core part of the micelles.[41] The halo corresponds to the shell composed of alkyl chains, which are less densely packed. Since no such clear core−shell boundary is observed for the bigger spheres, they could correspond to aggregates of smaller micellar particles. On the other hand, the TEM images of polyTCDM (Figure 5c and 5d) show hollow structures or vesicles in the size range of 0.6−2.5 μm. Figure 5c shows a circular image with a dark ring separating a light core from a shell of smeared periphery of hairlike strands extending from 100 to 350 nm. The dark ring corresponds to a collapsed polymer backbone composed of alkyl units and the lighter core corresponds to solvent-filled cavities. PolyTCDM with its higher solubility leads to the formation of solvent-filled vesicles which swell the backbone of alkyl chains which explains the observed thickness of the shell. The smeared periphery suggests deformation of the spherical vesicle at the point of its contact with the Formvar support. However, at present it is very difficult to confirm the exact origin of the long hairlike strands extending outward from the ring, and X-ray

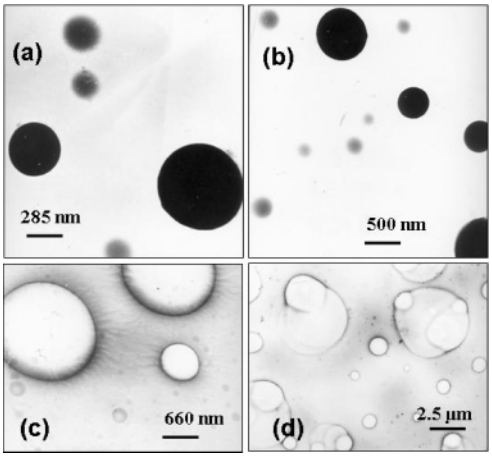

Figure 5. TEM images of polyAdM (a and b) and polyTCDM (c and d) prepared via free radically. The films were prepared by drop-casting polymer solution (10 mg/mL) of THF:water (9:1 v/v).

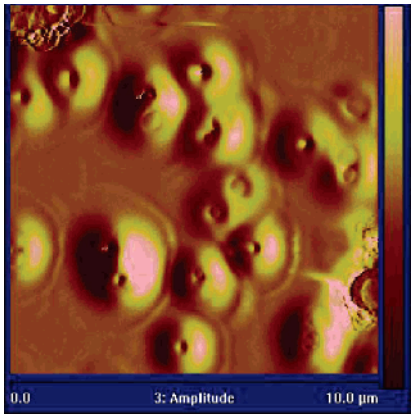

Figure 6. AFM image of a 10^{-6} M solution of polyTCDM in THF: H_2O = 9:1 v/v polymerized free radically.

diffraction studies may be very useful to get more insight. Recently, Ding and Liu had reported the formation of hairy vesicles from polyisoprene-*block*-poly(2-cinnamoylethyl methacrylate) where TEM images revealed a circular image consisting of a dark ring separating a light core from a shell of intermediate darkness. They explained the observation as solvent plasticized vesicles where the lighter center corresponded to solvent-filled cavities which swelled the polyisoprene chains and the dark ring represented collapsed polyisoprene layers.[42] Therefore, in the present case also TEM morphology observed for the novel TCDM-based bulky methacrylate polymers is similar to that observed in the literature. Some of the vesicles were found to fuse to form larger vesicles, the driving force behind the fusion process being the release of strain in the initially formed vesicles. In the case of polyTCDM, both TEM and SEM observations show similar results for the average pore diameters which are in the same range (see Table 2). In the case of polyAdM, the TEM shows particles of much smaller dimensions. However, it is a known fact that during evaporation of samples on the grid for TEM measurements, aggregation of particles, chain collapse, deformation, and so forth can take place thereby making an accurate estimation of size and size distribution quite difficult.[41] The observed difference in the structure formation of polyTCDM (hollow spheres) and polyAdM (filled spheres) could be attributed to the higher rigidity and lesser solubility of the adamantane system compared to the tricyclodecane system which could, in turn, lead to a different hydrophilic/hydrophobic balance. Jenekhe and Chen[31] have shown that for rod−coil diblock copolymers, effective packing of the rigid block facilitates the formation of aggregates with a central cavity. They have shown for a rod−coil system based on poly(phenylquinoline)-*block*-polystyrene that the same system in two different selective solvents can self-organize into two qualitatively different particles: hollow hard spheres and hollow soft spheres. Similarly, in our case, the difference in rigidity and solubility of the TCDM and AdM system results in hollow and filled structures, respectively, as observed by the TEM micrographs.The vesicular nature of the polyTCDM samples is further confirmed by tapping-mode atomic force microscopic (AFM) pictures (Figure 6) taken of a 10^{-6} M solution of the sample in THF:water = 9:1 v/v drop-cast on mica substrate. The morphologies exhibit collapsed hollow spheres.[43] Despite the wide difference in concentration of sample used for SEM, TEM (10^{-2} M), and AFM (10^{-6} M) measurements, the AFM pictures of polyTCDM clearly shows the formation of uniform vesicles of pore size in the range 1−2 μm similar to that observed by TEM.

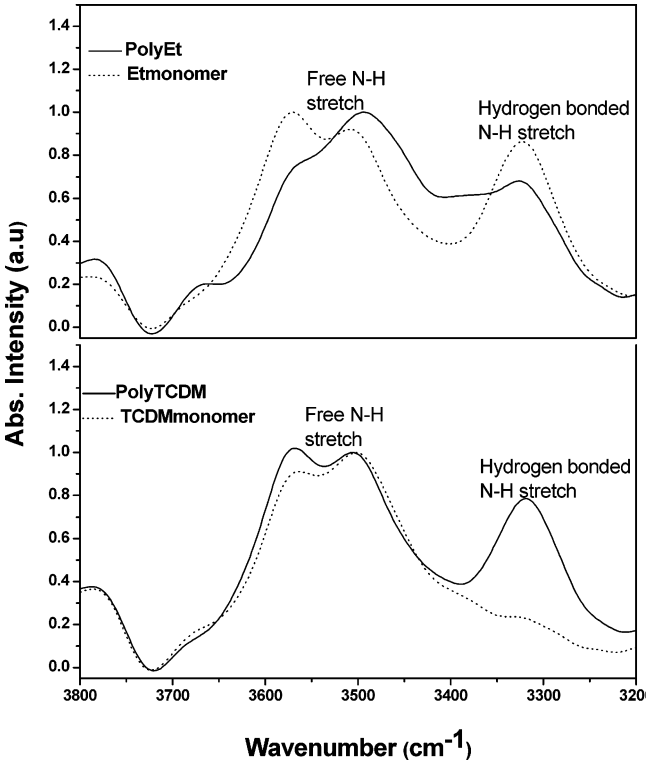

Figure 7. Normalized FT-IR spectra (expanded N−H region) of Et-monomer, polyEt, TCDM-monomer, and polyTCDM.

FTIR spectroscopy can be effectively used to understand the hydrogen bond characterization and to distinguish between hydrogen-bonded and free N−H and carbonyl stretching vibrations of the urethane linkage. Figure 7 shows the normalized expanded region of the N−H stretching vibration for Et-monomer and its polymer and TCDM-monomer and its polymer in THF. The two bands at higher wavenumbers (3570 and 3505 cm^{-1}) are assigned to the free antisymmetric and symmetric stretching vibrations of the N−H group in the urethane linkage, respectively.[44,45] The band at lower wavenumber (3319 cm^{-1}) is assigned to the hydrogen-bonded N−H stretching vibration. For all cases, the spectra are normalized with respect to the free N−H stretching vibrations. By comparing the intensities of the hydrogen-bonded N−H peaks for the polymer and monomer, respectively, it can be seen that in the case of TCDM there is an increase in the intensity of the hydrogen-bonded N−H peak upon polymerization. In the case of Et, there is a slight decrease in the intensity of the hydrogen-bonded N−H peak upon polymerization. This is direct evidence to the fact that in our unique monomer design when the terminals are substituted with bulky units, self-organization brought about by hydrogen bonding of the urethane linkage plays an important role in shaping the morphology of the polymer. It also stresses the uniqueness of our monomer design having both hydrogen-bonding linkage as well as bulky terminal unit incorporated into the same system. The thermal stability of the system was established using TGA. The 10% weight loss temperatures for the ATRP samples are given in Table 1. It shows the higher thermal stability of the polyTCDM and polyAdM samples compared to the others. In conclusion, the micropore formation observed for these polymers could be attributed to a combined effect of breath-figure mechanism as well as self-organization arising from hydrogen bonding. In these systems, the combination of rigidity versus flexibility and hydrophilicity versus hydrophobicity is just right to be able to facilitate the self-organizing forces of the hydrogen-bonding urethane linkages,

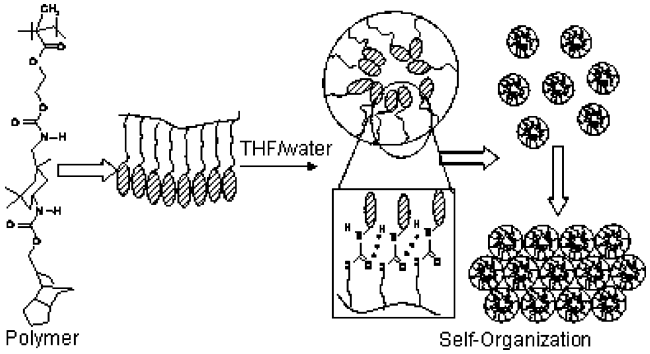

Figure 8. Schematic representation showing the contribution of self-organization brought about by hydrogen bonding toward the microporous pattern formation.

which can further assist in the effective packing of the rigid part. This is schematically illustrated in Figure 8. THF is a good solvent for the flexible polymer backbone, whereas it is a poor solvent for the bulky terminal. Therefore, in the THF:water = 9:1 solvent combination, one could expect a structure with the bulky terminals pointing inward away from the solvent outside, and this structure is retained in the solid state once the solvent evaporates. The urethane linkages help in stabilizing the structure formed by providing a means of strong intermolecular interaction through their hydrogen-bonding ability. There is also the probability that small amounts of water can assist in self-organization via hydrogen bonding with the urethane groups. However, one can rule out that this is the major driving force for pore formation, since in that case one would have expected pore formation in polyEt and polyDec also in the presence of THF:water 9:1, which is not the case here.

Conclusion

The notable feature of the polymers illustrated here is the unique molecular design involving manipulation of supramolecular architecture and hydrophilic/hydrophobic balance, which has clearly demonstrated that the honeycomb porous film formation usually associated only with rod−coil block polymers or star polymers is more a morphology driven process than mere water droplets condensing to form a template. The presence of either one factor alone, hydrogen-bonding linkage or bulky terminal unit, is not sufficient condition for producing well-ordered structures as evidenced by the absence of any special structural features in films prepared under identical conditions for the control polymer (having bulky unit but no hydrogen-bonding linkage and ethylene oxy unit) or for polyEt and polyDec (having hydrogen-bonding linkage and ethyleneoxy linkage but no bulky terminal). Additionally, this work also demonstrates that honeycomb formation from these polymers occurs over a wide molecular weight window as well as large polydispersity indices as evidenced by the pore formation from both the normal free radical polymerized as well as ATRP samples. This work adds a new dimension to the structural diversity of polymers that are known to form honeycomb microporous films.

Acknowledgment. We thank Celanese Chemical Co. for providing tricyclodecane methanol as a research sample for this fundamental research. We thank the Kerala State Council for Science, Technology, & Environment (KSCSTE), Trivandium, Kerala, India (030/SRSPS/2005/CSTE) and the Council of Scientific & Industrial Research (CSIR), New Delhi, India (Task Force Project, COR0004) for financial support. We thank Dr. Peter Koshy and Mr. M. R. Chandran RRL-Trivandrum for SEM and Dr. Suresh Das and Robert Philip, RRL-Trivandrum for AFM analysis. We also thank Dr Annie John, SCTIMST, Trivandrum for TEM analysis. V. D. Deepak thanks CSIR-New Delhi, India for Junior Research Fellowship.

Supporting Information Available: SEC plot, SEM photograph, ^{1}H and ^{13}C NMR spectra, and TGA plot. This material is available free of charge via the Internet at http://pubs.acs.org.

References and Notes

(1) de Boer, B.; Stalmach, U.; van Hutten, P. F.; Melzer, C.; Krasnikov, V. V.; Hadziioannou, G. *Polymer* **2001**, *42*, 9097.
(2) de Boer, B.; Stalmach, U.; Melzer, C.; Hadziioannou, G. *Synth. Met.* **2001**, *121*, 1541.
(3) Joannopouios, J. D.; Meade, R. D.; Winn, J. N. *Photonic Crystals: Molding the Flow of Light*; Princeton University Press: Princeton, NJ, 1995.
(4) Martin, C. R. *Science* **1994**, *266*, 1961.
(5) Gasparac, R.; Kohli, P.; Paulino, M. O. M.; Trofin, L.; Martin, C. R. *Nano Lett.* **2004**, *4*, 513.
(6) Campbell, M.; Sharp, D. N.; Harrison, M. T.; Denning, R. G.; Turberfield, A. J. *Nature* **2000**, *404*, 53.
(7) Nicolau, D. V.; Yaguchi, T.; Iguchi, H.; Yoshikawa, S. *Langmuir* **1999**, *15*, 3845.
(8) Bhatia, S. K.; Hickman, J. J.; Ligler, F. S. *J. Am. Chem. Soc.* **1992**, *114*, 4432.
(9) Pitois, O.; Francois, B. *Colloid Polym. Sci.* **1999**, *277*, 574.
(10) Widawski, G.; Rawiso, M.; Francois, B. *Nature* **1994**, *369*, 387.
(11) Srinivasarao, M.; Collings, D.; Philips, A.; Patel, S. *Science* **2001**, *292*, 79.
(12) Govor, L. V.; Bashmakov, I. A.; Kaputski, F. N.; Pientka, M.; Parisi, J. *Macromol. Chem. Phys.* **2000**, *201*, 2721.
(13) Govor, L. V.; Bashmakov, I. A.; Kiebooms, R.; Dyakonov, V.; Parisi, J. *Adv. Mater.* **2001**, *13* (8), 588.
(14) Karthaus, O.; Maruyama, N.; Cieren, X.; Shimomura, M.; Hasegawa, H.; Hashimoto, T. *Langmuir* **2000**, *16* (15), 6071.
(15) Pitois, O.; Francois, B. *Eur. Phys. J. B* **1999**, *8*, 225.
(16) Francois, B.; Pitois, O.; Francois, J. *Adv. Mater.* **1995**, *7*, 1041.
(17) Nishikawa, T.; Nishida, J.; Ookura, R.; Nishimura, S.; Wada, S.; Karino, T.; Shimomura, M. *Mater. Sci. Eng. C* **1999**, *10*, 141.
(18) Nishikawa, T.; Ookura, R.; Nishida, J.; Sawadaishi, T.; Shimomura, M. *RIKEN Rev.* **2001**, *37*, 43.
(19) Stenzel-Rosenbaum, M. H.; Davis, T. P.; Fane, A. G.; Chen, V. *Angew. Chem., Int. Ed.* **2001**, *40*, 3428.
(20) Wang, Y.; Liu, Z.; Huang, Y.; Han, B.; Yan, G. *Langmuir* **2006**, *22*, 1928.
(21) Park, M. S.; Kim, J. K. *Langmuir* **2004**, *20*, 5347.
(22) Jenekhe, S. A.; Chen, X. L. *Science* **1999**, *283*, 372.
(23) de Boer, B.; Stalmach, U.; Nijland, H.; Hadziioannou, G. *Adv. Mater.* **2000**, *12*, 1581.
(24) Hayakawa, T.; Horiuchi, S. *Angew. Chem., Int. Ed.* **2003**, *42*, 2285.
(25) Stenzel, M. H. *Aust. J. Chem.* **2002**, *55*, 239.
(26) Bolognesi, A.; Mercogliano, C.; Yunus, S. *Langmuir* **2005**, *21*, 3480.
(27) Lee, M.; Cho, B.; Ihn, K. J.; Lee, W.; Oh, N.; Zin, W. *J. Am. Chem. Soc.* **2001**, *123*, 4647.
(28) Li, Z.; Zhao, W.; Liu, Y.; Rafailovich, M. H.; Sokolov, J. *J. Am. Chem. Soc.* **1996**, *118*, 10892.
(29) Mu, M.; Ning, F.; Jiang, M.; Chen, D. *Langmuir* **2003**, *19*, 9994.
(30) Chen, D.; Jiang, M. *Acc. Chem. Res.* **2005**, *38*, 494.
(31) Jenekhe, S. A.; Chen, X. L. *Science* **1998**, *279*, 1903.
(32) Deepak, V. D.; Asha, S. K. *J. Polym. Sci., Part A: Polym. Chem.* **2006**, *44*, 4384.
(33) Deepa, P.; Jayakannan, M. *J. Polym. Sci., Part B: Polym. Phys.* **2006**, *44*, 1296.
(34) Asha, S. K.; Deepthimol, V.; Lekshmi, M. *J. Polym. Sci., Part A: Polym. Chem.* **2004**, *42*, 5617.
(35) Beers, K. L.; Boo, S.; Gaynor, S. G.; Matyjaszewski, K. *Macromolecules* **1999**, *32*, 5772.
(36) Zhou, P.; Chen, G. Q.; Hong, H.; Su, F. S.; Li, Z. C.; Li, F. M. *Macromolecules* **2000**, *33*, 1948.
(37) The molecular weights of polyTCDM and polyAdM polymerized using ATRP route deviated from that of the calculated value of M_n, which might be due to the bulky nature of the terminating group. Further studies are ongoing to analyze the effect of the bulky group on the kinetic parameters of controlled radical polymerization.
(38) Bormashenko, E.; Pogreb, R.; Stanevsky, O.; Bormashenko, Y.; Gendelman, O. *Mater. Lett.* **2005**, *59*, 3553.
(39) Lin, C. L.; Tung, P. H.; Chang, F. C. *Polymer* **2005**, *46*, 9304.

(40) Hao, X.; Stenzel, M. H.; Barner-Kowollik, C.; Davis, T. P.; Evans, E. *Polymer* **2004**, *45*, 7401.
(41) Wang, M.; Zhang, G.; Chen, D.; Jiang, M.; Liu, S. *Macromolecules* **2001**, *34*, 7172.
(42) Ding, J.; Liu, G. *Chem. Mater.* **1998**, *10*, 537.
(43) Duan, H.; Chen, D.; Jiang, M.; Gan, W.; Li, S.; Wang, M.; Gong, J. *J. Am. Chem. Soc.* **2001**, *123*, 12097.
(44) Furer, V. L. *J. Mol. Struct.* **2000**, *520*, 117.
(45) Asha, S. K.; Schenning, A. P. H. J.; Meijer, E. W. *Chem.—Eur. J.* **2002**, *8*, 3353.